Singlet Excited State Dynamics of Tetrakis(4-*N*-methylpyridyl)porphine Associated with DNA Nucleotides

Ravi Jasuja,[†] David M. Jameson,[‡] Coreen K. Nishijo,[†] and Randy W. Larsen*,[†]

Department of Chemistry and Department of Biochemistry and Biophysics, University of Hawaii at Manoa, Honolulu, Hawaii 96822

Received: August 30, 1996; In Final Form: December 3, 1996[⊗]

The singlet excited state behavior of tetrakis(4-*N*-methylpyridyl)porphine (T4MPyP) in the presence of the four mononucleotides of DNA in aqueous solution has been examined. Addition of the nucleotides of adenine, thymine, or cytosine to a solution containing T4MPyP results in an increase in the fluorescence intensity of the porphyrin, while addition of guanine substantially quenches the intensity. Optical absorption measurements demonstrate noncovalent interactions of the nucleotides with the porphyrin, resulting in bathochromic shifts in the Soret region. Binding constants for the base:porphyrin complexes were determined from steady-state absorption data to be 1743 ± 68, 385 ± 15, 2433 ± 150, and 198 ± 7 M^{-1} for dAMP, dTMP, dGMP, and dCMP, respectively. The T4MPyP singlet state lifetime increases from 5.29 to 11.3, 10.3, and 7.8 ns in the presence of dAMP, dTMP, and dCMP, respectively. In the case of dGMP, the lifetime data was best fit to a Lorentzian distribution centered at 0.69 ns and a discrete component at 3 ns. The quenching was modeled using an excited state reaction mechanism coupled with ground state complexation. The quenching is attributed to electron transfer between guanine (the most reducing of the bases) and T4MPyP (i.e., reductive quenching of the porphyrin singlet state).

Introduction

The use of porphyrins as photosensitizers has long been recognized as an effective cancer therapy.[1–3] One mechanism of action involves the generation of singlet oxygen via energy transfer from a long-lived triplet excited state of porphyrin.[4] An additional mode of oxidative damage to DNA, which has received considerable attention, is direct electron transfer from a base to a photoexcited chromophore, either intercalated or bound to the outside of DNA. One question of particular interest is whether there are specific sites to which oxidative damage migrates in DNA via electron transfer between various bases. Electron spin resonance studies have shown that radiolytic reduction of DNA causes negative charge to localize at cytosine while oxidation results in localized positive charge on guanine.[5]

Due to the success of porphyrins as photosensitizers, studies aimed at understanding the molecular interactions between porphyrins and DNA are of current interest. The interactions between free base and metalloderivatives of various mesosubstituted cationic porphyrins and various oligomers has been elucidated using UV−vis absorption, fluorescence, circular dichroism, and resonance Raman spectroscopies.[6–14] Intercalative binding of free base T4MPyP (Figure 1) and its planar metalloderivatives is preferred at GC-rich sequences and is characterized by a large bathochromic shift ($>$15 nm) in the Soret absorption band and an induced negative circular dichroism in the Soret region of T4MPyP. In addition, these interactions bring about a decrease in fluorescence intensity. On the other hand, outside binding at AT-rich sequences in DNA results in a smaller bathochromic shift in the Soret absorption band, an increase in fluorescence intensity, and an induced negative circular dichroism in the Soret region of T4MPyP.

While a majority of the studies involving porphyrin binding to DNA have been carried out using synthetic oligonucleotide sequences or natural DNA, molecular interactions between the
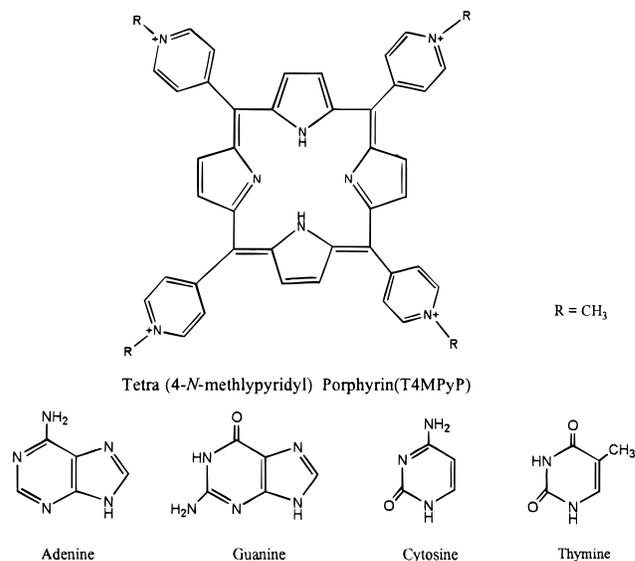

Figure 1. Structural diagrams of T4MPyP and DNA nucleosides used in this study.

ground and excited states of porphyrins with individual bases are not well understood. In studies using synthetic oligonucleotides or natural DNA, a cumulative effect of such interactions associated with the porphyrin binding site is examined, but the effect of individual bases cannot be isolated. However, Pasternack et al.[11] have demonstrated complex formation between cationic porphyrins and mononucleotides using optical spectroscopy and NMR techniques. In addition, redox studies involving photoactive intercalators and mononucleotides are currently being investigated by a number of research groups.[15–18] These efforts form a basis with which to probe excited state dynamics of cationic porphyrins complexed with mononucleotides as simple models for porphyrin:DNA interactions.

We have employed steady-state absorption and both steady-state and time-resolved fluorescence methods to probe the

interactions between individual nucleotides and the excited singlet state of T4MPyP. Interestingly, although dAMP and dGMP complexation to T4MPyP results in similar bathochromic shifts in the absorption spectra of T4MPyP (indicating $\pi-\pi$ stacking interactions), the interactions with the singlet excited state of T4MPyP are strinkingly different. Fluorescence of T4MPyP is highly quenched by dGMP. This quenching is described by a model in which an excited-state complex is deactivated via reductive quenching of the porphyrin singlet state. All other nucleotides including dAMP (which exhibits similar interactions with the T4MPyP ground state, as does dGMP) increase the fluorescence intensity. This increase in intensity has previously been observed in numerous instances of π-π complexation and is attributed to the exclusion of water molecules from the surface of the fluorophore (T4MPyP), thereby reducing the quenching and increasing the lifetime.

Materials and Methods

Nucleotides (sodium salts, Sigma) and T4MPyP (tosylate salt, Porphyrin products) were used as received. The stock solutions were prepared in 100 mM sodium phosphate ($\mu = 240$, no salt added) buffer (pH 7.1) to reduce the effects of changes in ionic strength during the course of the titrations. Absorption measurements were conducted using a quartz optical cuvette (1 cm optical path length) housed in a thermoelectrically modulated cell holder. The temperature for the titrations was maintained at 25 °C. Optical spectra were obtained using a Milton Roy Spectronic 3000 diode array spectrophotometer. A 2 mL solution containing 10 μM T4MPyP in phosphate buffer was used for the absorption titrations, and spectra were recorded subsequent to each addition of nucleotide stock solution (15 mM). At this concentration, T4MPyP has been found to be monomeric.[11] Absorption spectra were monitored as a function of ionic strength by adding NaCl. Concentrations of NaCl were increased up to 0.75 M and changes in absorption maxima were recorded in terms of position as well as intensity. All the spectra were corrected for dilution before any further manipulations of the data were performed.

Binding constants for complex formation were determined using the following equation

$$1/\Delta A = 1/([L]K_{eq}(\Delta A)_i) + 1/(\Delta A)_i \qquad (1)$$

where [L] is the concentration of added nucleotide, ΔA is the change in absorbance after each addition of nucleotide to the porphyrin solution, ΔA_i represents the extrapolated change in absorbance at infinite nucleotide concentration, and K_{eq} is the equilibrium constant for complex formation.

Steady-state fluorescence measurements were performed using an SLM 8000C spectrofluorometer (SLM Aminco, Champaign, IL) equipped with a red sensitive Hamamatsu R928 photomultiplier tube and data acquisition software from ISS (ISS, Inc., Champaign, IL). Samples were excited at 437 nm (isosbestic point in the absorption titrations), and the fluorescence of T4MPyP was viewed through a Schott RG082 filter which passes wavelengths greater than 570 nm. For the quenching experiments with dGMP, the concentration of dGMP (starting at 11.2 mM) was reduced successively while keeping the concentration of T4MPyP (5 μM) constant.

Time-resolved fluorescence was obtained using an ISS K2 multifrequency and phase modulation spectrofluorometer. Excitation of each sample was accomplished using the 488 nm line from an argon ion laser (Spectra-Physics model 2045). We note that although T4MPyP has a low extinction coefficient at 488 nm, there is still ample excitation with the laser to result in

a strong fluorescence signal. The resulting emission above 570 nm was observed through a Schott RG082 cutoff filter. The exciting light was polarized parallel to the vertical laboratory axis, while the emission was viewed through a polarizer oriented at 55° (to eliminate bias in lifetime measurements due to polarization effects).[19]

The multifrequency phase and modulation approach for time-resolved fluorescence relies on intensity modulation of the excitation source, and the phase shift and relative modulation of the emitted light, with respect to the excitation, are determined.[19-21] Lifetimes are then calculated according to the equations

$$\tan(P) = \omega \tau^P$$

$$M = [1 + (\omega \tau^M)^2]^{-1/2}$$

where P is the phase shift, M is the relative modulation (the ac/dc ratios of the excitation and emission wave forms), and ω is the angular modulation frequency. Two independent lifetime determinations, τ^P and τ^M, are thus obtained. An emitting system characterized by a single-exponential decay will yield identical phase and modulation lifetime values irrespective of the modulation frequency. In the case of heterogeneous emitting systems (multiple noninteracting fluorescent species), the phase liftime will be less than the modulation lifetime and those values will furthermore be dependent upon the modulation frequency, namely, decreasing as the modulation frequency increases.[20-25] The measured phase and modulation values may be analyzed as a sum of exponentials by using a nonlinear least-squares procedure[21,25] wherein the goodness of fit to a particular model (for example, single or double exponential) is judged by the value of the reduced chi-square (χ^2) as defined by

$$\chi^2 = \sum \{(P_c - P_m/\sigma^P) + (M_c - M_m/\sigma^M)\}/(2n - f1)$$

where the sum is carried out over the measured values at n modulation frequencies and f is the number of free parameters. The symbols P and M correspond to the phase shift and relative demodulation values, respectively, while the indices c and m indicate the calculated and measured values, respectively. σ^P and σ^M correspond to the standard deviations of each phase and modulation measurement, respectively. The calculated values of phase and modulation are obtained using the equations previously described.[22,25]

Results

Absorption Titration Studies. In the absence of nucleotides, the absorption spectrum of T4MPyP displays a Soret maximum at 422 nm (Figure 2, panel a). Bathochromic shifts in the Soret band are observed upon addition of various nucleotides resulting in a single isosbestic point (see Table 1), indicating the presence of only two absorbing species in equilibrium. A representative example of the difference spectra (dGMP/T4MPyP) is displayed in Figure 2, panel b. Difference spectra were obtained by subtracting the uncomplexed T4MPyP spectrum from the T4MPyP spectrum in the presence of nucleotides corrected for dilution. Examination of the bathochromic shift in the Soret absorption of T4MPyP as a function of nucleotide concentration reveals the extent of complex formation since the nucleotides do not absorb beyond 300 nm. Excellent fits to eq 1 were obtained assuming a 1:1 stoichiometry for the complexes (for example, Figure 2, panel b). The values of the association constants are similar to, but distinct from, those reported by Pasternack et al.[11] However, we note that the experiments in this study were carried out in solutions containing 100 mM
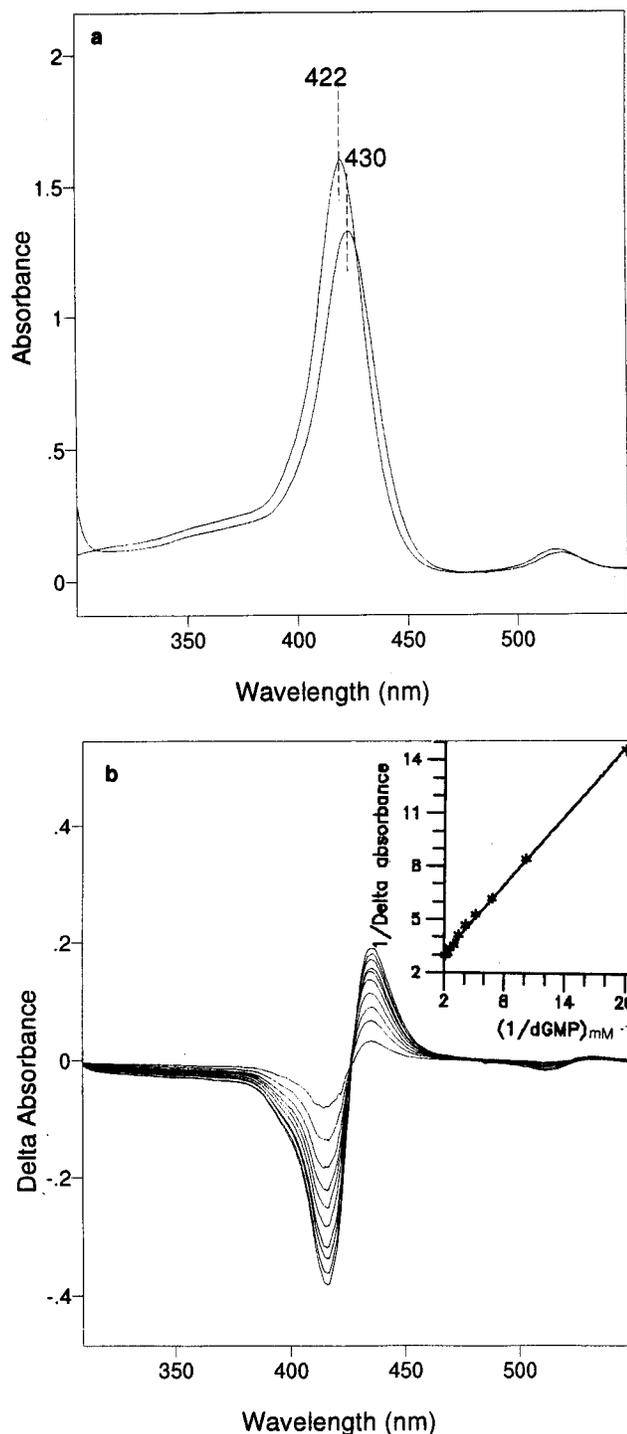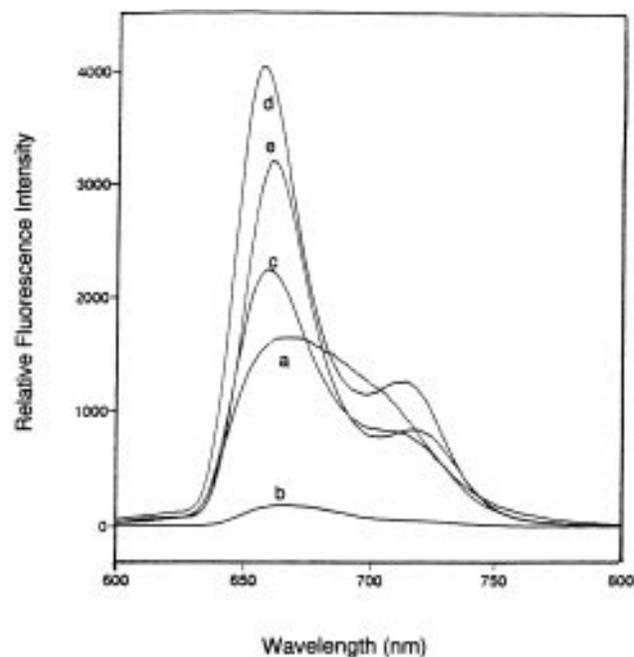
Figure 3. Steady-state fluorescence spectra for (a) T4MPyP (10 μM) with (b) dGMP, (c) dCMP, (d) dAMP, and (e) dTMP nucleotide/ T4MPyP > 1000; λ_{ex} = 488 nm.

phosphate buffer and up to 10 mM concentrations of the sodium salts of the corresponding nucleotides. Such high concentrations of nucleotides may lead to significant changes in solution ionic strength and affect the association constant values. It is not clear that such effects have been accounted for in the earlier work.

Steady-State and Time-Resolved Fluorescence Studies. The steady-state fluorescence spectra of T4MPyP, free and in the presence of various nucleotides, are shown in Figure 3. In the absence of nucleotide, the emission spectrum of T4MPyP is broad and extends from ~600 to ~800 nm. Upon addition of either dAMP, dCMP, or dTMP, the T4MPyP emission band increases in intensity and displays two very distinct peaks centered at 653 and 714 nm. Addition of dGMP, however, results in a significant quenching of the porphyrin fluorescence, while the general shape of the emission spectrum is unchanged.

The quenching data can be analyzed using the Stern−Volmer method.[26] The Stern−Volmer equation is

$$I_0/I = 1 + k^*\tau_0[q] \qquad (2)$$

where I and I_0 are the fluorescence intensities observed in the presence and absence of quencher, respectively, k^* is the bimolecular quenching constant, τ_0 is the lifetime in the absence of the quencher, and [q] is the quencher concentration. In the case of purely dynamic quenching, i.e., quenching solely by collisional deactivation of the singlet excited state, a Stern−Volmer plot of I_0/I versus [q] yields a straight line. Upward curvature in Stern−Volmer plots results when complex formation (static quenching) occurs accompanied by dynamic quenching.[27] In such cases a modified Stern−Volmer equation can be utilized which explicitly includes a static quenching (non-emissive complex) component due to complex formation

$$I_0/I = (1 + K_a[q]) (1 + k^*\tau_0[q]) \qquad (3)$$

where K_a is the association constant of the complex between fluorophore and quencher.

For cases where ground state association between quencher and fluorophore lead to an emissive complex, eq 3 can be further

Figure 2. Panel a: optical absorption spectra of T4MPyP in the absence (I, top) and presence (II, bottom) of dGMP. Porphyrin concentration is 10 μM dGMP, 2 mM in 100 mM phosphate buffer, pH 7.1. Spectra were obtained using a 1 cm quartz optical cell. Panel b: absorption difference spectra of T4MPyP (10μM) titrated with dGMP (final concentration 0.47 mM). Inset is a fit for eq 1 for 1:1 association stoichiometry of the complex.

TABLE 1: Effect of Complexation on the Absorption Spectra

nucleotide	$\Delta\lambda$ (nm)	binding constant (M^{-1})
dGMP	12	2433 ± 150
dAMP	13	1743 ± 68
dCMP	3	198 ± 7
dTMP	2	385 ± 15

phosphate buffer, pH 7.1 (ionic strength, μ = 240 mM), while data reported by Pasternack et al.[11] was obtained using 8 mM

Dynamics of Tetrakis(4-*N*-methylpyridyl)porphine

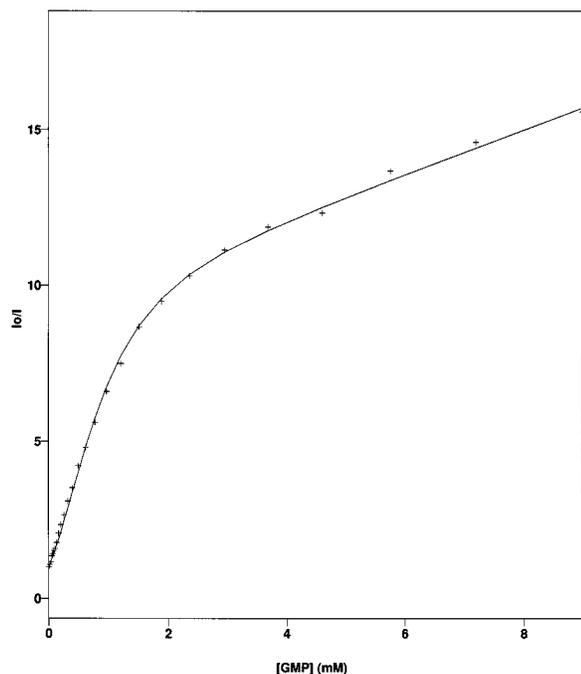*J. Phys. Chem. B, Vol. 101, No. 8, 1997* **1447**

Figure 4. Stern–Volmer plot for the quenching of fluorescence of T4MPyP (10 μM) by dGMP (final concentration 22 mM) and the corresponding fit to the eq 4.

modified to include the fluorescence contributions from the free and as well as the complexed fluorophore

$$I_0/I = (1 + K_a[q])\,(1 + \tau_1 k_{q1}[q])/(1 + [(\tau_1/\tau_2)K_a[q](1 + \tau_1 k_{q1}[q])/(1 + \tau_2 k_{q2}[q])]) \quad (4)$$

where K_a is the ground state association constant and k_{q1} and k_{q2} are the quenching rates for the free and the complexed fluorophore by unbound quencher.[28–31]

The Stern–Volmer plots (Figure 4) for the quenching of T4MPyP singlet excited state by dGMP exhibit a downward curvature consistent with an emissive complex formation. The data were fit to eq 4 by fixing the lifetime of the free fluorophore (τ_1) to 5.29 ns and the binding constant to 2433 M^{-1}. The quenching rates (k_{q1} and k_{q2}) and the lifetime of the complex were determined from the resulting fit to be $(7.32 \pm 2) \times 10^{11}$ M^{-1} s^{-1}, $(2.4 \pm 0.1) \times 10^{12}$ M^{-1} s^{-1}, and 0.12 ns, respectively. The quenching constants are considerably larger than would be expected for simple diffusional quenching. An estimate of the diffusional quenching constant can be obtained using the Debye formula[28]

$$k_d = 8NKTb/3000\eta(e^b - 1) \quad (5)$$

where η is the coefficient of viscosity of the solvent, b is the collision distance for the two species, N is Avogadro's number, and K is the Boltzmann constant. The number obtained from the calculation is ~1×10^9 M^{-1} s^{-1}. Previous studies of Ru-(II)tris(bipyridine) excited state quenching by various anions give similar quenching constants and are attributed to activation controlled quenching processes.[28]

Singlet lifetime measurements were performed at high nucleotide to porphyrin ratios (>1000) to minimize the contribution from uncomplexed porphyrin. The results are summarized in Figure 5 and in Table 2. In the case of dAMP, dCMP, and dTMP, the phase data were best fit to a sum of two exponential decays and the longer lifetime component was attributed to the complexed T4MPyP. The fit of the dGMP lifetime data, however, was significantly improved using a
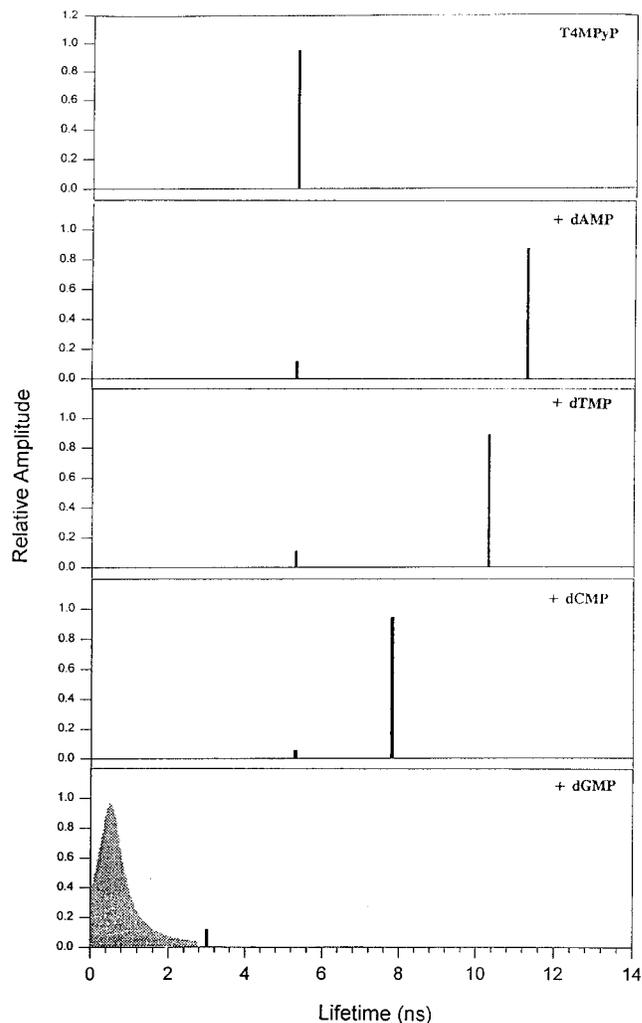

Figure 5. Fluorescence lifetime distributions for T4MPyP (10 μM) in the absence and presence of various nucleotides at high nucleotide/porphyrin ratios (>1000).

TABLE 2: Effect of Complexation on the Fluorescence Lifetimes

nucleotide	component 1 τ_1 (ns)	fraction 1	component 2 τ_2 (ns)	fraction 2	χ-square
none	5.29	1			3.5
dAMP	5.29[b]	0.119	11.27	0.881	2.0
dGMP	3.0	0.12	0.69[a]	0.88	2.3
dCMP	5.29[b]	0.056	7.8	0.944	0.8
dTMP	5.29[b]	0.111	10.3	0.889	2.7

[a] Center of Lorentzian distribution of lifetimes with fwhm of 0.93 ns. [b] Corresponds to the lifetime of free T4MPyP fixed during analysis.

Lorentzian distribution model (see Discussion section). The data obtained from dGMP addition, however, could not be fit to a discrete exponential decay scheme with an acceptable χ-square (see Discussion section). The lifetime of the complex also differs considerably from that obtained from the Stern–Volmer analysis. This is most likely due to the fact that the complex exhibits a distribution of lifetimes while the Stern–Volmer analysis assumes a discrete value.

Absorption and steady-state fluorescence experiments were repeated with the corresponding nucleosides, and similar trends in the fluorescence and absorption data were observed. However, for similar concentrations of nucleotides and nucleosides the changes in the fluorescence intensity and shifts in absorption maxima were less pronounced due to the addition of nucleosides. These differences in spectral perturbations are attributed to

weaker complexation with nucleosides due to the absence of negatively charged phosphate groups. Electrostatic contributions to the complex formation were confirmed by the recovery of the position and the intensity of the Soret absorption band of T4MPyP in the presence of nucelotides as the ionic strength of the solutions is increased.

Discussion

Effects of Complexation on Absorption Spectra. The changes in the absorption spectra of various electrostatic and $\pi-\pi$ complexes of metalloporphyrins with methyl viologens and phenanthrolines have been previously evaluated using the four-orbital model describing free-base and metalloporphyrins.[31−36] In the present case, T4MPyP complexation with nucleotides leads to electronic perturbations arising from solvent effects and dipole moment changes in the porphyrin macrocycle. Perturbations associated with changes in porphyrin solvent environment are likely to make a significant contribution to the overall spectral shift. In general, excited states arising from $\pi-\pi^*$ transitions such as the Soret transition are expected to decrease in energy as the solvent becomes increasingly hydrophobic, as a consequence of the large dipole moment associated with the $\pi-\pi^*$ excited state. The solvent perturbation arises from changes in the solvent−solute dipole interactions. Upon complexation, due to reduced exposure to water, the average energy of the unoccupied a_u and b_u orbitals decreases while the b_{2u} would increase slightly due the hydrophobic contact with DNA nucleotides. The resulting molecular parameters describing the configuration interactions are also affected. The $2A_g$ matrix element reflecting the splitting between the a_{2u} and b_{2u} orbitals should be raised in energy, while the A_g' matrix element should be reduced due to the solvent perturbation. The result would be a red shift in the Soret and visible region of complexed T4MPyP as compared to T4MPyP in aqueous solution. The difference in interactions between the nucleotides can be accounted for by the structural differences in the two groups of nucleotides. Both dGMP and dAMP (Figure 1) have a double-ring structure which leads to stronger $\pi-\pi$ interactions with T4MPyP and thus can more effectively remove water from the solvation shell of T4MPyP. On the other hand, dTMP and dCMP (Figure 1) have only single-ring structures effecting a comparatively weaker $\pi-\pi$ overlap upon complexation.

Effect of Complexation on Singlet Lifetimes and Fluorescence Spectra. Upon addition of dAMP, dTMP, and dCMP, changes in the fluorescence intensity and the shape of the emission band of T4MPyP are observed. The increase in intensity is consistent with $\pi-\pi$ complex formation between the nucleotides and T4MPyP since complexation is expected to exclude water molecules from the solvation shell of the porphyrin. This exclusion, in effect, reduces the collisional quenching of the singlet excited state of T4MPyP due to solvent molecules, thereby increasing the lifetime of the excited state in the complex. The broad fluorescence band of T4MPyP centered at 672 nm gives rise to two distinct bands centered at 653 and 714 nm upon addition of dAMP, dTMP, and dCMP. Similar changes in fluorescence band shape were reported due to the addition of CT-DNA to T4MPyP.[37] The splitting of the emission band of T4MPyP has also been reported in methanol.[39] This effect is attributed to the changes in the dielectric of the solvation sphere associated with the porphyrin. Complex formation with the nucleotides also results in similar effective dielectric changes by reducing the accessibility of the water molecules to the π orbitals of the porphyrin. In the case of dGMP, addition of the nucleotide to a solution containing T4MPyP causes substantial quenching of the fluorescence intensity.

The Stern−Volmer plot describing the quenching of T4MPyP by dGMP is linear at low dGMP concentrations and shows substantial downward curvature as the nucleotide concentration is increased. Such downward curvature in the Stern−Volmer plots has previously been reported for quenching reactions in which ground state association leads to the formation of a fluorescent complex.[28−30] Similar downward curvature for such plots has also been attributed to the decrease in activity of ionic reactants as a function of ionic strength. To avoid such effects, the ionic strength was maintained at 240 mM during the titrations using phosphate buffer. The rates of fluorescence quenching of both the porphyrin and the complex by dGMP are found to be faster than the natural decay rate for T4MPyP ($k_{nat} = 1.8 \times 10^8$ s^{-1}). These results from the fits to Stern−Volmer equation are consistent with the decay and quenching rates obtained with time-resolved fluorescence measurements with the exception of the complex lifetime. As stated above, one reason for the discrepancy in the lifetime of the complex obtained from time-resolved fluorescence and that obtained from the fit to the S−V equation is that we observe a distribution of quenched singlet lifetimes in the complex while the equation assumes a discrete rate for the static quenching.

As displayed in the Table 2, the T4MPyP, when complexed with either dAMP, dTMP, or dCMP, exhibited an increase in the singlet lifetime, and the data gave good fits to a biexponential decay model when the lifetime of one of the components was fixed at 5.29 ns (which corresponds to the lifetime of free T4MPyP). The increase in singlet lifetimes correspond to the relative increase in the fluorescence intensities for the addition of the three nucleotides. For the addition of dGMP, it was not possible to get reasonable fits for the lifetime data using discrete exponential decay schemes (either for two or three discrete decays).

Mechanism of Fluorescence Quenching by dGMP and Consequences on DNA Redox Properties. Electron transfer over long ranges through DNA has been demonstrated for several systems.[15−18,39−46] Purugganan et al.[45] used DNA-bound metal complexes of 1,10-phenanthroline as donor and acceptors to demonstrate electron transfer through the helix. Further, Murphy et al.[44] reported rapid photoinduced electron transfer between metallointercalators separated over 15 base pairs (>40 Å) in a DNA duplex. Both energy and electron transfer through DNA nucleotides have been observed by Brun and Harriman[40] between palladium porphyrins and other bound intercalators. Fewer studies have been conducted to understand the redox properties of photoactive intercalators and the nucleotides of DNA. Recently, Saito et al.[18] reported direct evidence for electron transfer from guanine to a photoexcited modified L-lysine residue. In addition, Shafirovich et al.[16] demonstrated that three of the DNA bases (guanine, thymine, and cytosine) quench the singlet excited state of benzo[a]pyrenetetraol. Interestingly, the direction of proton-coupled electron transfer from thymine and cytosine was reversed as compared to that with guanine.

In the present system, only the porphyrin is being excited ($\lambda_{ex} = 488$ nm) and the emission spectrum of T4MPyP does not overlap with the absorption spectrum of the dGMP. Therefore, energy transfer from T4MPyP to the nucleotide cannot be an acceptable mechanism for quenching. Examination of redox potentials of the nucleotides and the T4MPyP demonstrate that the mechanism of singlet quenching most likely involves electron transfer between excited singlet of T4MPyP and dGMP.

The nature of the electron transfer pathway (i.e., oxidative or reductive quenching of the porphyrin singlet state) can be

Dynamics of Tetrakis(4-*N*-methylpyridyl)porphine

J. Phys. Chem. B, Vol. 101, No. 8, 1997 **1449**

understood by examining the free energy of the corresponding electron transfer reactions. For reductive quenching of the porphyrin, the thermodynamics of electron transfer from the nucleotide to the porphyrin can be calculated from the following equation[47]

$$\Delta G^\circ = e[E_b^\circ(\text{base/base}^{\bullet+}) - E_p^\circ(\text{T4MPyP*/T4MPyP}^{\bullet-})] - \Delta E_{00} + w$$

where w is the solvent reorganizational parameter, E_b° is the redox potential for nucleotide, E_p° is the reduction potential of the singlet excited state, and ΔE_{00} represents the energy of the singlet excited state of T4MPyP. $E_b^\circ(\text{dGMP/dGMP}^{\bullet+})$, E_b°-$(\text{dTMP/dTMP}^{\bullet+})$, $E_b^\circ(\text{dCMP/dCMP}^{\bullet+})$, and $E_b^\circ(\text{dAMP/dAMP}^{\bullet+})$ are 1.53, 1.73, 1.88 and 1.94 V, respectively, and $E_p^\circ(\text{T4MPyP*/}$ T4MPyP$^{\bullet-})$ is -0.23 V (all the values are vs NHE).[48,49] The excited singlet state energy (ΔE_{00}) for the porphyrin is 1.83 eV. Thus, a thermodynamically favorable electron transfer from the base to the excited T4MPyP will be anticipated only when $E^\circ(\text{nucleotide/nucleotide}^{\bullet+})$ is less than 1.60 V. Only dGMP is expected to reduce the singlet excited state of the T4MPyP with $\Delta E_{net} = +0.07$ V ($\Delta G = -6.76$ kJ/mol). The corresponding oxidative quenching reaction (i.e., electron transfer from T4MPyP to dGMP) can be described thermodynamically using a similar equation:

$$\Delta G^\circ = e[E^\circ(\text{T4MPyP*/T4MPyP}^{\bullet+}) - E^\circ(\text{base/base}^{\bullet-})] - \Delta E_{00} + w$$

The estimated redox potential for (dGMP/dGMP$^{\bullet-}$) is -2.7 V and for (T4MPyP*/T4MPyP$^{\bullet+}$) is $+0.34$ V. From these values, the possibility of oxidative quenching of T4MpyP can be eliminated since the radical ion-pair has higher energy than the energy of the singlet excited state of T4MPyP. Thus it is suggested that observed quenching reaction involves electron transfer from guanine to T4MPyP.

Of specific interest is the fact that the singlet lifetime of T4MPyP is not a discrete component in the presence of dGMP but rather fits best to a distribution of lifetimes centered at 0.69 ns. This is in contrast to the singlet lifetimes previously reported[38] using natural DNA where two discrete lifetimes were found (2.0 ± 0.5, 10.0 ± 0.5). It is not evident if the authors fit data for the shorter lifetime component using the distribution function. In the present study, however, the distribution of lifetimes implies a distribution of electron transfer rates between the singlet excited state of T4MPyP and dGMP within the complex. The origin of this distribution can be understood by examining the expression for the electron transfer rate constant derived from semiclassical Marcus theory. The following equation describes the rate constant for nonadiabatic electron transfer between two redox centers held at a constant distance[50]

$$k_{et} = \nu_N k_E \exp[-(\Delta G + \lambda)^2/4\lambda RT]$$

where ν_N is the frequency of motion along the reaction coordinate, k_E describes electronic coupling between the redox centers and is a function of donor/acceptor orientation and separation distance, λ is the total reorganizational energy (including inner-sphere and outer-sphere contributions), and ΔG is free energy of the reaction. Since the complex between dGMP and T4MPyP is not expected to be rigid in solution, conformational flexibility is anticipated which results in a distribution of relative orientations of electric dipoles between dGMP and T4MpyP. This distribution will be reflected in the

SCHEME 1
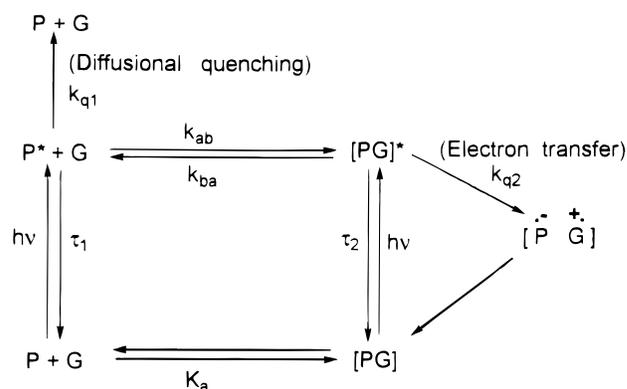
electron transfer rates since some orientations may result in more effective dipole coupling than other geometries, thus, in effect, varying k_E.

Scheme 1 depicts a mechanism of quenching of T4MPyP via electron transfer based upon the absorption and fluorescence data presented above. In this scheme P, G, and [PG] represent T4MPyP, dGMP, and the T4MPyP:dGMP complex, respectively, K_a is ground state association constant, τ_1 and τ_2 are the singlet state lifetimes for the free and complexed T4MPyP, respectively, and k_{q1} and k_{q2} are the corresponding quenching constants. The data obtained here gives $\tau_1 = 5.29$ ns, $K_a = 2433$ M^{-1}, $k_{q1} = 3 \times 10^{11}$ M^{-1} s^{-1} (3 ns component from time-resolved fluorescence data scaled to base concentration), and $k_{q2} = 1.8 \times 10^9$ s^{-1} (Note that this is the center of the distribution of quenched lifetimes and is distinct from k_{q2} determined from the Stern−Volmer analysis). The value for τ_2 could not be determined since only the statically (Lorentzian distribution centered at 0.69 ns) and dynamically (3 ns component) quenched lifetimes could be observed.[51] However, this implies that τ_2 must be longer than 3 ns. The values for k_{ab} and k_{ba} also could not be determined, but it is expected that the equilibrium constant in the excited state is similar to that in the ground state suggesting that $k_{ab}/k_{ba} \sim 2400$ M^{-1}.

Significance to DNA:T4MPyP Complexes. Previous studies[37] of T4MPyP with CT DNA and synthetic oligonucleotides have shown that intercalative binding at GC-rich regions leads to reduced fluorescence emission while outside binding at AT-rich regions results in an increase in emission intensity. The current data demonstrates that the interaction of either dAMP, dTMP, or dCMP with T4MPyP increases the lifetime of the singlet excited state of T4MPyP resulting in increased fluorescence intensity. In addition, these interactions cause a splitting of the emission band of T4MPyP similar to that observed for T4MPyP binding to poly[d(A-T)]. The decrease in intensity associated with intercalation of T4MPyP with GC regions is now shown to be due to thermodynamically favored electron transfer from G to the excited singlet state of T4MPyP.

In summary, the data presented here demonstrate that T4MPyP forms complexes with the four nucleotides of DNA and that quenching of the singlet excited state of T4MPyP occurs only in the presence of dGMP. The quenching reaction is shown to be reductive with a forward electron transfer rate on the order of 10^9 s^{-1} and a back rate on the same or faster time scales. In addition, significant orientational dependence is observed resulting in a distribution of quenched lifetimes. Together these results form a basis for enhancing our understanding of electron transfer between porphyrins and DNA and lay a foundation for investigation of the conformational dynamics associated with photoinduced charge migration in porphyrin/oligonucleotide complexes.

References and Notes

(1) Hilf, R. Cellular Targets of Photodynamic Therapy as a Guide to Mechanisms. In *Photodynamic Therapy: Basic Principles and Clinical Applications*; Henederson, B. W., Dougherty, T. J., Eds.; Marcel Dekker Inc.: New York, 1992.

(2) Dubbelman, T. M. A. R.; Prinsze, C.; Penning, L. C.; Steveninck, J. V. Photodynamic Therapy: Membrane and Enzyme Photobiology in *Photodynamic Therapy: Basic Principles and Clinical Applications*; Henederson, B. W.; Dougherty, T. J., Eds.; Marcel Dekker Inc.: New York, 1992.

(3) Dougherty, T. J. *Photochem. Photobiol.* **1987**, *45*, 879−889.

(4) Spikes, J. D. *Ann. N.Y. Acad. Sci.* **1975**, *244*, 496.

(5) Fiel, R. J. *J. Biomol. Struct. Dyn.* **1989**, *6*, 1259.

(6) Feng, Y.; Pilbrow, J. R. *Biophys. Chem.* **1990**, *36*, 117−131.

(7) Carvlin, M. J.; Fiel, R. J. *Nucleic Acids Res.* **1983**, *11*, 6121−6139.

(8) Yue, K. T.; Lin, M.; Gray, T. A.; Marzilli, L. G. *Inorg. Chem.* **1991**, *30*, 3214−3222.

(9) Carvlin, M. J.; Mark, E.; Fiel, R. J.; Howard, J. C.; *Nucleic Acids Res.* **1983**, *11*, 6141−6154.

(10) Sari, M. A.; Battoni, J. P.; Dupre, D.; Mansuy, D.; Le Pecq, J. B. *Biochem. Pharmacol.* **1988**, *37*, 1861.

(11) Pasternack, R. F.; Gibbs, E. J.; Gaudemer, A.; Antebi, A.; Bassner, S.; DePoy, L.; Turner, D. H.; Williams, A.; Laplace, F.; Lansard, M. H.; Merienne, C.; Perree-Fauvet, M. *J. Am. Chem. Soc.* **1985**, *107*, 8179−8185.

(12) Fiel, R. J.; Howard, J. C.; Mark, E. H.; Datta Gupta, N. *Nucleic Acids Res.* **1979**, *6*, 3093−3118.

(13) Pasternack, R. F.; Gibbs, E. J.; Villafranca, J. J. *Biochemistry* **1983**, *22*, 2406−2414.

(14) Pasternack, R. F.; Brigandi, R. A.; Abrams, M. J.; Williams, A. P.; Gibbs, E. J. *Inorg. Chem.* **1990**, *29*, 4483−4486.

(15) Tuite, E.; Kelly, J. M.; Beddard, G. S.; Reid, G. S. *Chem. Phys. Lett.* **1994**, 517−524.

(16) Shafirovich, V. Ya.; Courtney, S. H.; Naiqi, Y.; Geacintov, N. E. *J. Am. Chem. Soc.* **1995**, *117*, 4920−4929.

(17) Armitage, B.; Yu, C.; Devados, C.; Schuster, G. B. *J. Am. Chem. Soc.* **1994**, *116*, 9847−9859.

(18) Saito, I.; Takayama, M.; Sugiyama, H.; Nakatani, K. *J. Am. Chem. Soc.* **1995**, *117*, 6406−6407.

(19) Spencer, R. D.; Weber, G. *J. Phys. Chem.* **1970**, *52*, 1654−1663.

(20) Spencer, R. D.; Weber, G. *Ann. N.Y. Acad. Sci.* **1969**, *158*, 361.

(21) Bismuto, E.; Jameson, D. M.; Gratton, E. *J. Am. Chem. Soc.* **1987**, *109*, 2354−2357.

(22) Jameson, D. M.; Hazlett, T. L. Time-Resolved Fluorescence in Biology and Biochemistry. In *Biophysical and Biochemical Aspects of Fluorescence Spectroscopy*; Dewey, T. G., Ed.; Plenum Press: New York, 1991; pp 105−133.

(23) Lakowicz, J. R. *J. Biophys. Biochem. Methods* **1980**, *2*, 91.

(24) Jameson, D. M.; Gratton, E.; Hall, R. D. *App. Spectrosc. Rev.* **1984**, *20*, 55−105.

(25) Larsen, R. W.; Jasuja, R.; Hetzler, R. K.; Muraoka, P.; Andrada, V. G.; Jameson, D. M. *Biophys. J.* **1996**, *70*, 443−452.

(26) Stern, O.; Volmer, M. *Z. Phys.* **1919**, *20*, 183.

(27) Vaughan, W. M.; Weber, G. *Biochemistry* **1970**, *9* (3), 464−473.

(28) Rybak, W.; Halm, A.; Netzel, T.; Sutin, N. *J. Phys. Chem.* **1981**, *85*, 2856−2860.

(29) White, H. S.; Becker, W. G.; Bard, A. J. *J. Phys. Chem.* **1984**, *88*, 1840−1846.

(30) Rybak, W.; Halm, A.; Netzel, T. L.; Sutin, N. *J. Phys. Chem.* **1981**, *85*, 2856−2860.

(31) Basu, S.; Paul, T. K.; Ray, S. *Indian J. Chem.* **1989**, *28A*, 729−734.

(32) Shellnut, J. A. *J. Phys. Chem.* **1984**, *88*, 6121−6127.

(33) Gouterman, M. *J. Chem. Phys.* **1959**, *30*, 1139−1161.

(34) Gouterman, M. *J. Mol. Spectrosc.* **1961**, *6*, 138−163.

(35) Seybold, P. G.; Gouterman, M. *J. Mol. Spectrosc.* **1969**, *31*, 1−13.

(36) Shellnut, J. A. *J. Phys. Chem.* **1984**, *88*, 4988−4992.

(37) (a) Kelly, J. M.; Murphy, M. J.; McConnell, D. J.; OhUigin, C. *Nucleic Acids Res.* **1985**, *13*, 167−184. (b) Liu, Y.; Konigstein, J. A.; Yevdokimov, Y. *Can. J. Chem.* **1991**, *69*, 1791−1795.

(38) Vergeldt, F. J.; Koehorst, R. B. M.; Hoek, A. V.; Schaafsma, T. J. *J. Phys. Chem.* **1995**, *99*, 4397−4405.

(39) Brun, A. M.; Harriman, A. *J. Am. Chem. Soc.* **1994**, *116*, 10383−10393.

(40) Fromherz, P.; Rieger, B. *J. Am. Chem. Soc.* **1986**, *108*, 5361−5362.

(41) Brun, A. M.; Harriman, A. *J. Am. Chem. Soc.* **1992**, *114*, 3656−3660.

(42) Candeias, L. P.; Steenken, S. *J. Am. Chem. Soc.* **1993**, *115*, 2437−2440.

(43) Murphy, C. J.; Arkin, M. R.; Jenkins, Y.; Ghatlia, N. D.; Bossman, S. H.; Turro, N. J.; Barton, J. K. *Science* **1993**, *262*, 1025−1029.

(44) Purugganan, M. D.; Kumar, C. V.; Turro, N. J.; Barton, J. K. *Science* **1988**, *241*, 1645−1649.

(45) Lecomte, J. P.; Kirsch-De Mesmaeker, A.; Kelly, J., M.; Tossy, A. B.; Gorner, H. *Photochem. Photobiol.* **1992**, *55*, 681−689.

(46) Rehm, D.; Weller, A. *Isr. J. Chem.* **1970**, *8*, 259.

(47) Kittler, L.; Lober, G.; Gollmock, F. A.; Berg, H. *Bioelectrochem. Bioenerg.* **1980**, *7*, 503.

(48) Kalyanasundaram, K.; Neumann-Spallart, M. *J. Phys. Chem.* **1982**, *86*, 5163−5169.

(49) Kalyanasundaram, K. *Inorg. Chem.* **1984**, *23*, 2453−2459.

(50) Marcus, R. A.; Sutin, N. *Biochem. Biophys. Acta* **1985**, *811*, 265.

(51) Triplet state diffusional quenching was also observed with increasing dGMP concentration (Jasuja and Larsen, unpublished results). But within the complex, electron transfer is very efficient and takes place via quenching of the T4MPyP singlet excited state since at high (∼10 mM) dGMP concentrations; no triplet excited state of T4MPyP was detected.